The phase-2 upgrade of the CMS Resistive Plate Chamber system

General Scientific Meeting 2016 of the Belgian Physical Society

Alexis Fagot

in behalf of the CMS RPC community

Ghent University - Department of Physics and Astronomy

alexis.fagot@ugent.be

The Compact Muon Solenoid

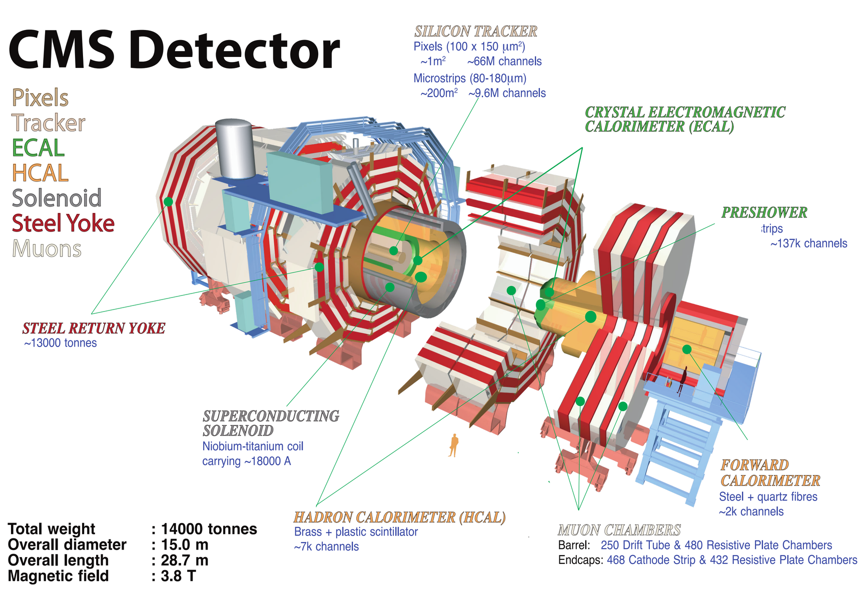

Figure 1 : Exploded view of the CMS detector.

CMS is a multipurpose physics detector (Fig. 1) located on the Large Hadron Collider (LHC) whose main feature is a superconducting solenoid of $6\ \mathrm{m}$ diameter containing a silicon pixel and strip tracker, a PbW cristal ECAL and a HCAL composed of Brass and scintillating material. Outside the magnet, gas detectors, among which RPCs (Fig. 2), embedded in the return yokes compose the muon system [1]. The CMS barrel is closed by 2 endcaps.

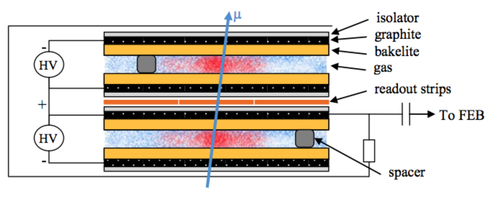

Figure 2 : Schematics of a RPC as used in CMS. Muons are detected by gas amplification.

Motivations for the upgrade

After the third long shutdown (LS3), LHC will enter a high luminosity period called HL-LHC or Phase-2. The instantaneous luminosity will be raised to $5 \times 10^{34}\ \mathrm{cm^{-2}s^{-1}}$ and the event pile-up will become a major challenge for experiments like CMS [2].

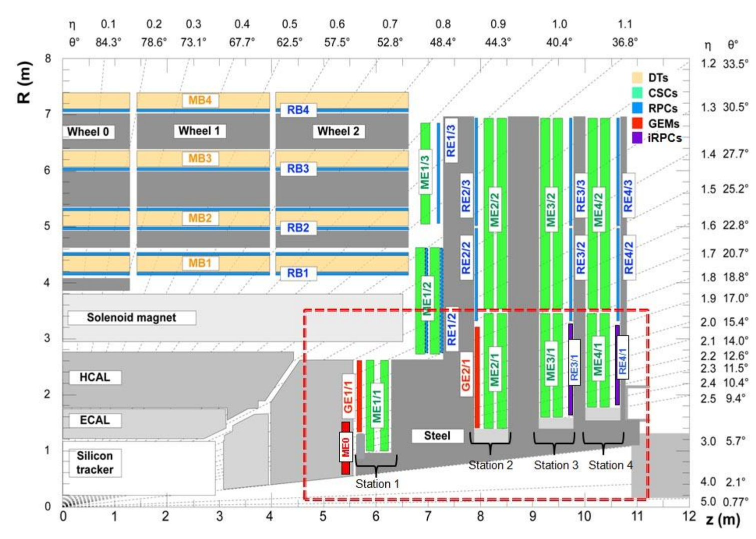

Figure 3 : Quadrant of the muon system showing DT chambers (yellow), RPC (light blue), and CSC (green). Phase-II forward muon detectors are contained within the dashed box : in red for GEM stations and dark blue for improved RPC (iRPC) stations.

Close to the beam line, an increased background is expected [3]. R&D teams are working on proposing solutions to equip a third endcap disk closer to the beam to increase the redundancy of the level-1 trigger (Fig. 3). The expected rate in RPC stations RE3/1 and RE4/1 is around $0.6\ \mathrm{kHz/cm^2}$ for a total integrated charge of $1\ \mathrm{C/cm^2}$ over a period of $T_{eff} = 6 \times 10^7\ \mathrm{s}$ (Fig. 4).

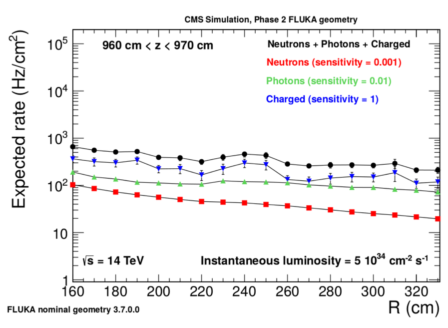

Figure 4 : Simulated particle hit rate as a function of radius at the RE3/1 station (0.001 sensitivity to n, 0.01 to γ & 1 to ionizing particles).

Prototypes will be tested in a new Gamma Irradiation Facility (GIF++) combining a $100\ \mathrm{GeV}$ μ beam and a $14\ \mathrm{TBq}$ ^{137}Cs source. Assuming a mean charge per avalanche of $20\ \mathrm{pC}$ and an acceleration factor AF=2, the needed irradiation time is about 17 months.

$$\left.\begin{array}{r} Q_{int}^{HL-LHC} = \langle q \rangle \cdot T_{eff} \cdot \Phi_{eff} \\ Q_{int}^{GIF} = \langle q \rangle \cdot T_{irr} \cdot \Phi_{eff} \cdot AF \end{array}\right\} \Leftrightarrow T_{irr} = \frac{T_{eff}}{AF}$$

Forward RPC technologies

In the perspective of HL-LHC, it is needed to produce RPCs that can handle high rates. As they are resistive detectors, increasing the rate capability through a reduction of its electrodes resistivity is a natural solution.

Electrode material	$\rho(\Omega\mathrm{cm})$	Institutes
HPL	$0.5-1\times10^{10}$	INFN[4]
LRS glass	10^{10}	IPNL-LLR-Tsinghua[5][6]
Vanadate glass	10^4 to 10^{16}	Coe College-ANL-University of Iowa[7]
SiC based ceramics	10^7 to 10^{12}	HZDR[8]
Ferrite ceramics	10^6 to 10^{13}	CSIC-USC[9]

Table 1 : Low resistivity materials list used for iRPC prototypes.

Changing the electrode resistivity alone won't help in reducing the ageing effects due to the amount of deposited charge per avalanche created in the gas gap. Reducing this mean charge deposition will lead to reduce the total integrated charge over long periods. This can be achieved via more sensitive low noise front end electronics (Fig. 5).

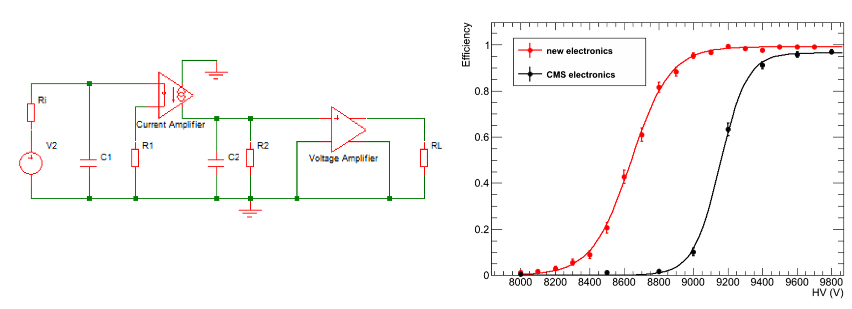

Figure 5 : Block diagram of ATLAS amplifier. R1: impedance resistance (left). Efficiency plateaus for standard CMS RPC FEE and new ATLAS prototype electronics (right). A shift of $\sim 460\ \mathrm{V}$ is observed corresponding to a decrease of charge deposition from $20\ \mathrm{pC}$ to $3\ \mathrm{pC}$.

Choosing a better performing RPC design, with optimized electrode or gas gap thickness and various number of gaps, to combine with the previously presented FEE prototypes can be investigated to further reduce the mean charge deposition per avalanche and thus the charge recombination time and the related detector dead time (Fig. 6).

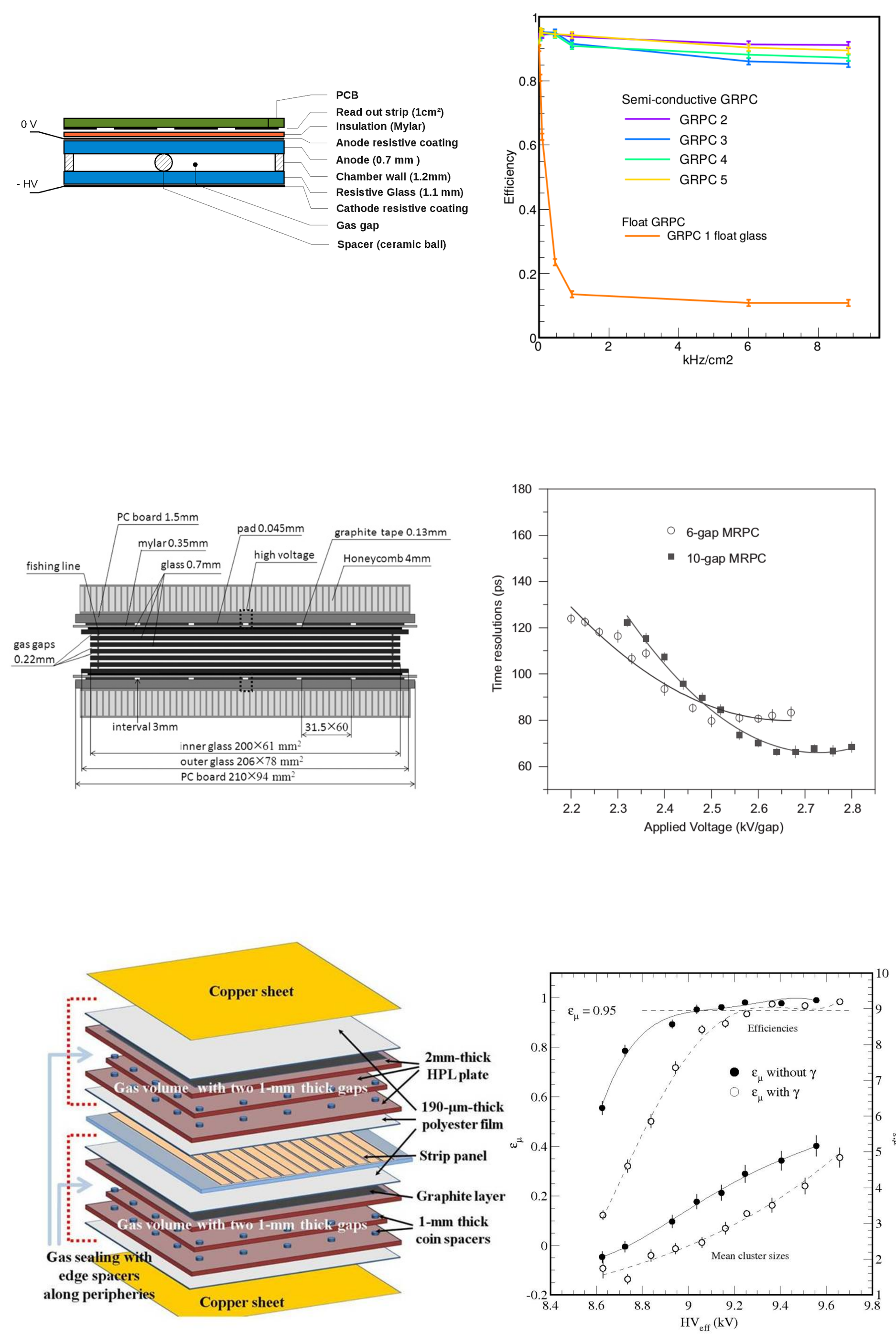

Figure 6 : Schematics of a RPC with electrodes made of low resistive silicate glass or float glass together with the efficiency vs rate for different RPCs [5] (top). 6-gap RPC together with time resolution as a function of HV (incoming μ-rate of $1.2\ \mathrm{kHz/cm^2}$) [6](center). Multigap HPL RPC prototype together with efficiency plateau and cluster size as function of HV w/ (open symbols) and w/o (solid symbols) a $3\ \mathrm{kHz/cm^2}$ γ-irradiation [4] (bottom).

Preliminary results

Figure 7 : Schematics of CMS endcap RPC. It is made of 3 RPC gaps called Top Wide (TW), Top Narrow (TN) and Bottom (Bot) and the readout is divided into 3 pseudo-rapidity strip partitions called A, B and C.

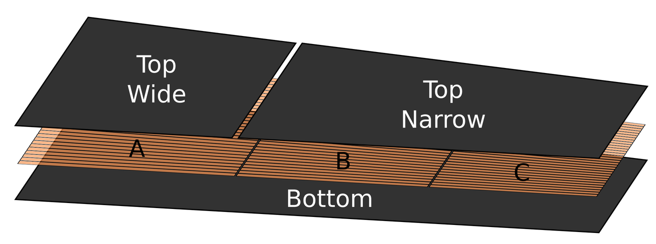

In the GIF++, the fully opened source gives a current of $2.6 \cdot 10^6 \gamma\ \mathrm{cm^{-2}s^{-1}}$. The performance of the RPCs are measured with a DAQ system and analysed at different values of attenuation of the γ flux.

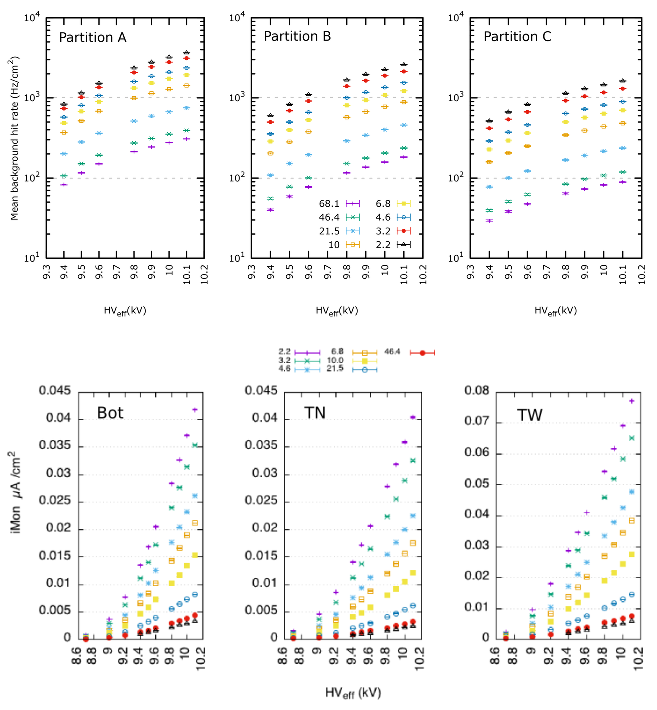

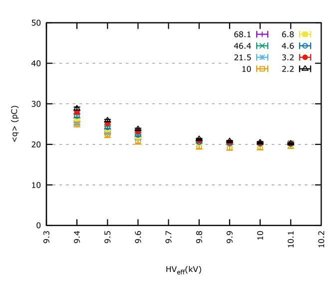

Figure 8 : Mean γ-hit rate (top left), current (bottom) and corresponding charge deposition (top right) as a function of HV_{eff} in chamber RE2-2-NPD-BARC-8 exposed to γ-irradiation for different values of attenuation).

To understand potential ageing effects, it is necessary to have a good measure of rates, currents and efficiency (Fig. 8 - 9) and to monitor through time the total integrated charge (Fig. 10). Hit rates are normalised to the strip size and currents to the gap area.

Figure 9 : Maximum efficiency as a function of the maximal mean background hit rate. T1S1 is RE2-2-NPD-BARC-8, T1S2 is RE2-2-NPD-BARC-9, T1S3 is RE2-2-CERN-166, T1S4 is RE2-2-CERN-165

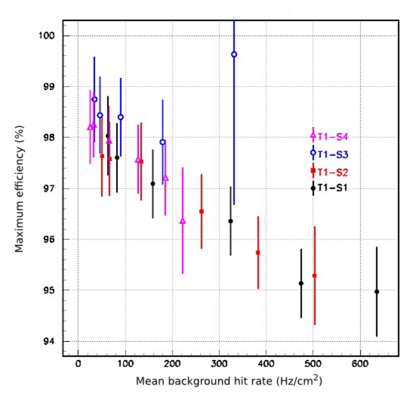

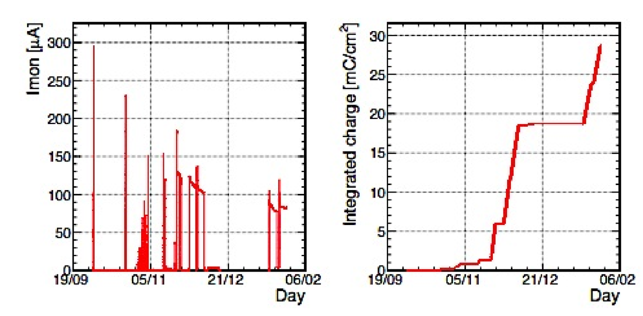

Figure 10 : Monitored current (left) and total integrated charge (right) for an ageing test of 87 days on chamber RE2-2-PK-140 in 2015-2016 at the new GIF++.

Conclusions

The RPC community is moving forward into conceiving and testing new RPC prototypes. The final technique adopted for the next upgrade may combine the benefits of the different R&D approaches. Although, it is needed to urgently address the issue of the installation of RE3/1 and RE4/1 in LS3. Finally, the first GIF++ test beam results are appearing and will need to be followed with attention.

[1] CERN. Geneva. LHC Experiments Committee. CMS, the Compact Muon Solenoid : technical proposal. Technical report, CMS Collaboration, 1994.

[2] CERN. Geneva. LHC Experiments Committee. Technical Proposal for the Phase-II Upgrade of the CMS Detector. Technical report, CMS Collaboration, 2015.

[3] S. Constantini. Radiation background with the CMS RPCs at the LHC. JINST, 2014.

[4] K. Lee. Rate capability study for a four-gap phenolic RPC with a Cs-137 source. JINST, 2014.

[5] Y. Haddad. High rate resistive plate chamber for LHC detector upgrades. Nucl. Instr. Meth. Phys. Res. A, 2013.

[6] J. Wang. Development of high-rate MRPCs for high resolution time-of-flight systems. Nucl. Instr. Meth. Phys. Res. A, 2013.

[7] N. Johnson. Electronically Conductive Vanadate Glasses for Resistive Plate Chamber Particle Detectors. IJAGS, 2015.

[8] A. Laso Garcia. Extreme high-rate capable timing resistive plate chambers with ceramic electrodes. JINST, 2012.

[9] M. Morales. Conductivity and charge depletion aging of resistive electrodes for high rate RPCs. JINST, 2013.